Control of Hopf Bifurcations in Hodgkin-Huxley Neurons by Automatic Temperature Manipulation

Reşat Özgür Doruk

ABSTRACT

The purpose of this research is to revisit the bifurcation control problem in Hodgkin-Huxley neurons. As a difference from the classical membrane potential feedback to manipulate the external current injection, we will actuate the temperature of the neural environment to control the bifurcations. In order to achieve this a linear feedback from the membrane potential is established to generate a time varying temperature profile. The considered bifurcating parameter is the external current injection. Upon finishing the controllers, the bifurcation analysis against the changes in external current injection is repeated in order to see the possibility of relapse of any bifurcation phenomena at nearby points. In addition to that, simulations are also provided to show the performances of the controllers.

Key Words: Hodgkin-Huxley Models, HopfBifurcation, Linear Feedback, Temperature Effects, MATCONT

DOI Number: 10.14704/nq.2018.16.2.1140 **NeuroQuantology 2018; 16(2):59-74**

Introduction

Hodgkin-Huxley model of the squid giant axon is a very important contribution to the field of theoretical neuroscience (Hodgkin & Huxley, 1952; Abbott, 2008). It is a highly nonlinear model of fourth order and exhibit various nonlinear phenomena especially the bifurcations (Crawford, 1991). Bifurcations in the nervous system might be an indicator of various neurological conditions (Milton *et al*., 1989) such as ankle clonus (Dimitrijevic *et al*., 1978), Parkinson's disease (Marsden, 1984; Marsden, 1984), seizures (Milton *et al*., 1987) related to the abnormal paroxysmal oscillations (Ayala *et al*., 1973) and bipolar disorders with rapid mood changes (Wehr& Goodwin, 1983). Some treatments such as anti-convulsant medications(Glaser *et al*., 1980), electro-convulsive therapies (Abrams, 2002) and biofeedback (Sterman & Friar, 1972; Forster, 1977) can be reflected as a bifurcation control task. Concerning bifurcation control there are numerous studies in the nonlinear systems literature. The most common control methodology is the washout filter (Doruk, 2010; Doruk, 2013; Hassouneh *et al*., 2004; Cheng, 2010; Ding & Hou, 2010; Lee & Abed, 1991) which is basically a high-pass filter which will allow the transients but block the steady states. This feature allows an action of bifurcation control without changing the equilibrium point of the bifurcation. This might be beneficial in neurological conditions as the equilibrium conditions are conserved. Other methods referring to the same problem are linear delayed feedback (Brandt & Chen, 1997; Peng, 2005, Liao *et al*., 2001; Zhou *et al.,* 2002; Cheng, 2010), nonlinear state feedback (Abed *et al*., 1992; Harb

Corresponding author: Reşat Özgür Doruk
Address: Department of Electrical and Electronic Engineering, Atilim University, Incek, Golbasi Ankara, Turkey
e-mail✉resat.doruk@atilim.edu.tr
Relevant conflicts of interest/financial disclosures: The authors declare that the research was conducted in the absence of any commercial or financial relationships that could be construed as a potential conflict of interest.
Received: 18 October 2017; **Accepted:** 2 January 2018

& Harb, 2004; Luo *et al*., 2003), harmonic balance approximation (Berns *et al*., 1998) and readjustment of quadratic invariants in normal form (Kang, 1998). Application of these methods to the control of bifurcation phenomena in Hodgkin-Huxley models can be met in (Doruk, 2010; Doruk, 2013; Hong, *et al*., 2012; Xie *et al.,* 2008; Wang *et al.,* 2007a; Wang *et al*., 2007b; Feudel *et al.,* 2000). In this work we will consider the same problem again but we will not employ a washout filter. Instead we establish a simple linear feedback from the membrane potential processed by a gain. The actuated input will be the temperature of the surrounding environment of the neuron. The bifurcating parameter is the external current injection I_{ext} and the analyses are performed using the command line version of MATCONT software (Dhooge *et al*., 2003). After choosing a feedback gain that stops the bifurcation the same analysis is repeated while the loop is closed to detect whether the bifurcation is repeating at a nearby position or not. Simulations are also performed to verify the research findings.

Methods

Hodgkin-Huxley (HH) Model

In this section, one is eligible to find a summary of the Hodgkin-Huxley model with its nominal parameters. It is a fourth order, highly nonlinear differential equation that exhibits a rich set of bifurcations. It is modeling the giant axon of a squid which has sodium, potassium and leakage (mostly due to chlorine) channels. Mathematical equations representing the model is:

$$\begin{aligned} C_m\frac{dV_m}{dt} &= -\bar{g}_K n^4(V_m-V_K)-\bar{g}_{Na}m^3h(V_m-V_{Na})-\bar{g}_l(V_m-V_l)+I_{ext} \\ \frac{dn}{dt} &= \alpha_n(V_m)(1-n)-\beta_n(V_m)n \\ \frac{dm}{dt} &= \alpha_m(V_m)(1-m)-\beta_m(V_m)m \\ \frac{dh}{dt} &= \alpha_h(V_m)(1-h)-\beta_h(V_m)h \end{aligned} \quad (1)$$

where V_m is the membrane potential in mV, n,m,h are dimensionless variables that stands for the potassium (K^+) channel activation, sodium (Na^+) channel activation and inactivation respectively. In other words they are the relative concentration of respective ions. They are in the interval [0,1]. The $\alpha_n(V_m)$, $\beta_n(V_m)$, $\alpha_m(V_m)$, $\beta_m(V_m)$, $\alpha_h(V_m)$ and $\beta_h(V_m)$ are functions of membrane potential as shown below:

$$\begin{aligned} &\alpha_n(V_m)=\frac{0.01(V_m+10)}{\exp(\frac{V_m+10}{10})-1} \quad \alpha_m(V_m)=\frac{0.1(V_m+25)}{\exp(\frac{V_m+25}{10})-1} \quad \alpha_h(V_m)=0.07\exp(\frac{V_m}{20}) \\ &\beta_n(V_m)=0.125\exp(\frac{V_m}{80}) \quad \beta_m(V_m)=4\exp(\frac{V_m}{18}) \quad \beta_h(V_m)=\frac{1}{\exp(\frac{V_m+30}{10})+1} \end{aligned} \quad (2)$$

The definitions and nominal values of the parameters are: $g_K = 36$ mS/cm^2 the conductance of the potassium channel, $g_{Na} = 120$ mS/cm^2 the conductance of the sodium channel, $g_l = 0.3$ mS/cm^2 the conductance of the channel representing leakage, $V_K = 36$ mV the equilibrium potential of the potassium channel, $V_{Na} = 115$ mV the equilibrium potential of the sodium channel and $V_l = 36$ mV the equilibrium potential of the channel representing leakage. In (1), I represents the current injected in mA/cm^2 from external sources (i.e. either a surrounding neuron or manual injection). When $I = 0$, one can see the response of the HH neuron with the nominal parameters in Figure 1.

When the temperature effects are considered, it will be convenient to apply (Fitzhugh, 1966; Rinberg *et al*., 2013) to the problem. Here, the temperature dependency of the ions (sodium,potassium and leakage ions like chlorine) are expressed as a factor η or ϕ:

$$\eta(T),\phi(T) = Q_{10}^{\frac{T-T_{ref}}{10}} \quad (3)$$

where T is the temperature of the neural environment in which will be the input to the neuron dynamics. The temperature T_{ref} is the temperature of the experimental environment where the original measurements of HH neuron are made. The value of this parameter is $T_{ref} = 6.3$. The value of the critical main parameter Q_{10} is 1.5 for conductances and 3 for the activation parameters α_i, β_i. The temperature effects are expressed by modifying the equation (1) as:

(1)

$$\begin{aligned} C_m\frac{dV_m}{dt} &= -\eta(T)\bar{g}_K n^4(V_m-V_K)-\eta(T)\bar{g}_{Na}m^3h(V_m-V_{Na})-\eta(T)\bar{g}_l(V_m-V_l)+I_{ext} \\ \frac{dn}{dt} &= \phi(T)\alpha_n(V_m)(1-n)-\phi(T)\beta_n(V_m)n \\ \frac{dm}{dt} &= \phi(T)\alpha_m(V_m)(1-m)-\phi(T)\beta_m(V_m)m \\ \frac{dh}{dt} &= \phi(T)\alpha_h(V_m)(1-h)-\phi(T)\beta_h(V_m)h \end{aligned} \quad (4)$$

In the above $\phi(T)$ is given by (3) with $Q_{10}=3$ and $\eta(T)$ is given by the same equation with $Q_{10}=1.5$.

Bifurcations in Dynamical Systems

In one sentence, bifurcation can be described as a phenomenon where a change in a parameter leads to qualitative changes in the response and characteristics of a nonlinear system. Both continuous time and discrete time systems exhibit this phenomena but they are termed different. For generic bifurcation discussion interested readers can refer to Scholarpedia (http://www.scholarpedia.org) and (Crawford, 1991). For the analysis of HH neurons (Doruk, 2010; Doruk, 2013) can be referred.

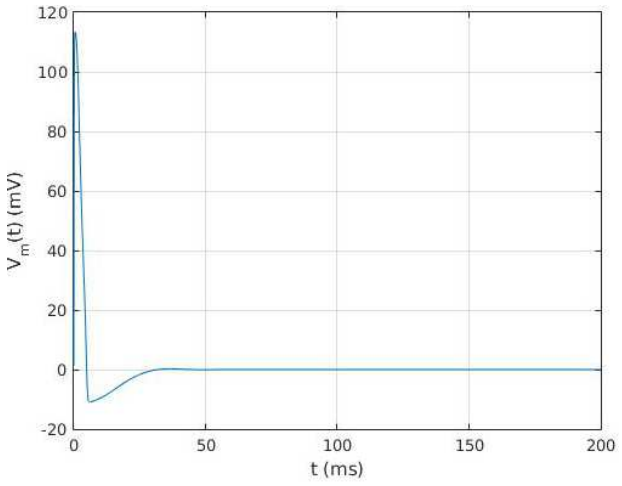

Figure 1. The response of HH model with the nominal values of parameters

In local bifurcation analysis, one should refer to the equilibrium points and the effected parameter. Consider a nonlinear dynamical system of the form:

$$\dot{x} = f(x, p) \quad (5)$$

where p is the bifurcated parameter. In addition, $f(x_q, p)=0$ where x_q is the equilibrium point at the onset of bifurcation.

Hopf Bifurcation (H)

Hopf bifurcation (Andronov *et al.,* 1973) a condition where a limit cycle erupts from an equilibrium in dynamical systems generated by ODEs. In this type of a bifurcation, the equilibrium changes stability via a pair of purely imaginary eigenvalues.

Limit Point (LP)

A limit point or saddle-node bifurcation (Kuznetsov, 2013) appears when two equilibria in a dynamical system collide and disappear. Mathematically speaking, this occurs when the critical equilibrium has one zero eigenvalue.

Neutral Saddle (NS)

Though not considered as a bifurcation, most bifurcation software such as MATCONT detects this as a critical point. A saddle point (Vidyasagar, 1978) is a situation where there are two eigenvalues of the Jacobian at the respective equilibrium point appear with opposite signs.

Results and Discussion

Bifurcation Analysis of the HH Neuron against injected current I_{ext}

Simulating (4) starting from the initial conditions $V_m(0)=0$, $n(0)=0$, $m(0)=0.3$ and $h(0)=0.7$ with $T=0$ will yield a stable steady state of $V_m(\infty)=0.0027$, $n(\infty)=0.3177$, $m(\infty)=0.0529$ and $h(\infty)=0.596$. Using the continuer module of the MATCONT software that is started from the given steady state will yield the bifurcation results presented in Table 1. The associated bifurcation diagram is shown in Figure 2. In order to obtain an insight of what is happening at these critical points one can see Figure 5 and Figure 8. In Figure 3 and 6 one can observe the response and trajectory of the membrane potential $V_m(t)$ (against time and potassium channel activation $n(t)$) resulting from a subcritical Hopf bifurcation condition in Table 1 Case 1 ($I_{ext}=6.686\,\mu$ A$/cm^2$). The non-decaying behavior of the response and the trajectories reveals the unstable nature of the erupted limit cycle. On the other hand, the supercritical Hopf case in the second column of Table 1 ($I_{ext}=118.351\,\mu$ A$/cm^2$) yielded a response and trajectory as shown in Figure 4 and Figure 7 which have a visible decaying behavior and reveals the stability of the erupted limit cycle.

Table 1. Results obtained from an analysis of single parameter bifurcation against the parameter I_{ext} of the HH equation in (4). The results are obtained from MATCONT software. The equilibrium values and respective eigenvalues at the condition of bifurcation are presented. The temperature related parameters are $\eta(T) = 0.7746$ and $\phi(T) = 0.5005$ which are evaluated at $T = 0$

Case	1	2
Par.	$I_{ext} = 6.686$	$I_{ext} = 118.351$
Equ.	$V_m = 4.903620$ $n = 0.394732$ $m = 0.092655$ $h = 0.421495$	$V_m = 21.847367$ $n = 0.642103$ $m = 0.417190$ $h = 0.071096$
Eig.	$\lambda_1 = -2.8079 + j0.0000$ $\lambda_2 = 0.0000 + j0.3440$ $\lambda_3 = 0.0000 - j0.3440$ $\lambda_4 = -0.0682 + j0.0000$	$\lambda_1 = -7.1555 + j0.0000$ $\lambda_2 = 0.0000 + j0.5600$ $\lambda_3 = 0.0000 - j0.5600$ $\lambda_4 = -0.1549 + j0.0000$
Cond.	Hopf	Hopf

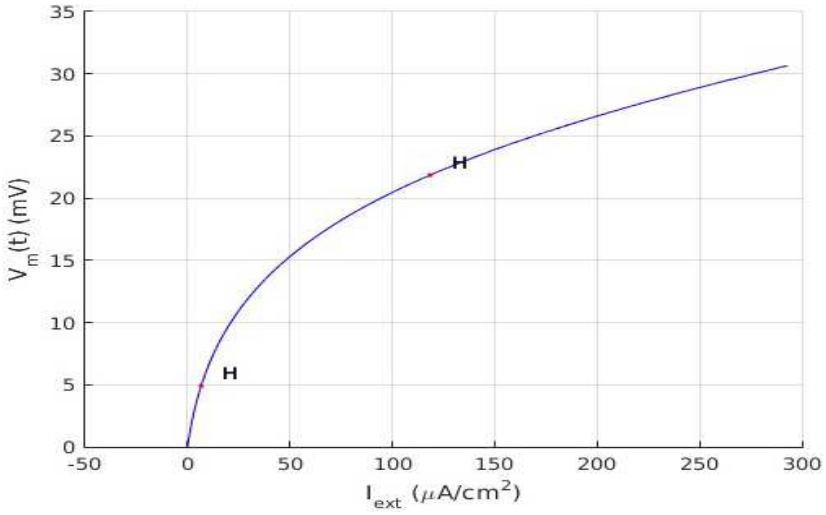

Figure 2. The bifurcation diagram of (4) against varying external current injection (I_{ext}). Two Hopf cases are noted at $I_{ext} = 6.686$ and $I_{ext} = 118.351$ μ A $/cm^2$.

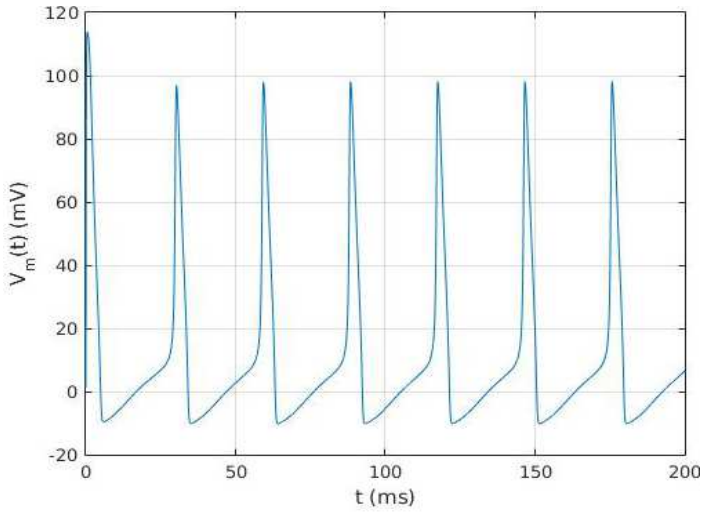

Figure 3a. Case 1: $I_{ext} = 6.686$

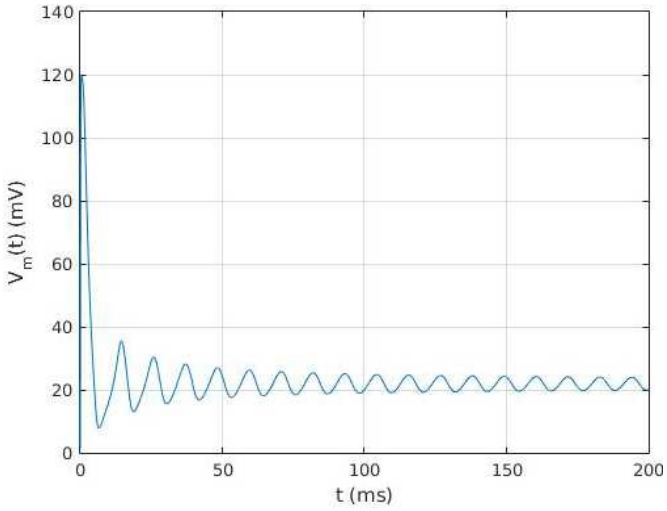

Figure 3b. Case 2: $I_{ext} = 118.351$

Figure 3. Uncontrolled simulation examples for two cases (1,2) from Table 1. In (a) a sustained oscillation is seen where as in (b) a decayed oscillation is seen. At the steady state there is a small amplitude oscillation which is expected from a Hopf bifurcation. This difference is also aligned with the criticality of bifurcation. Case 1 has a first order Lyapunov coefficient of 4.778256×10^{-3} which is positive thus the bifurcation is subcritical (limit cycle is unstable and thus has a higher possibility of diverging due to a small change in another parameter). Case 2 has a first order Lyapunov coefficient of -2.781224×10^{-3} which is negative thus the bifurcation is supercritical and its limit cycle is stable.

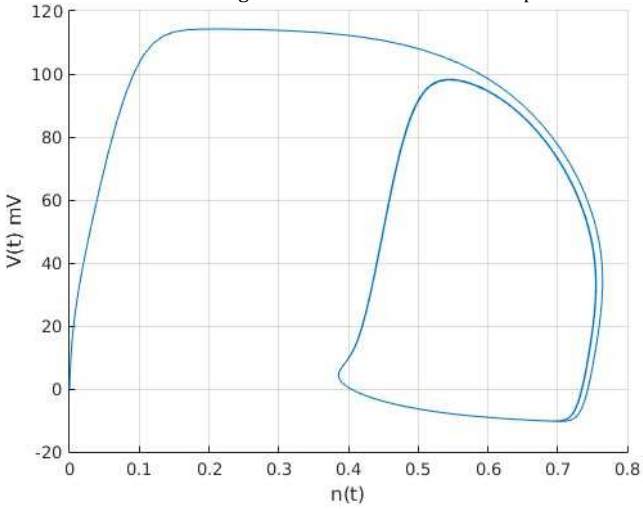

Figure 4a. Case 1: $I_{ext} = 6.686$

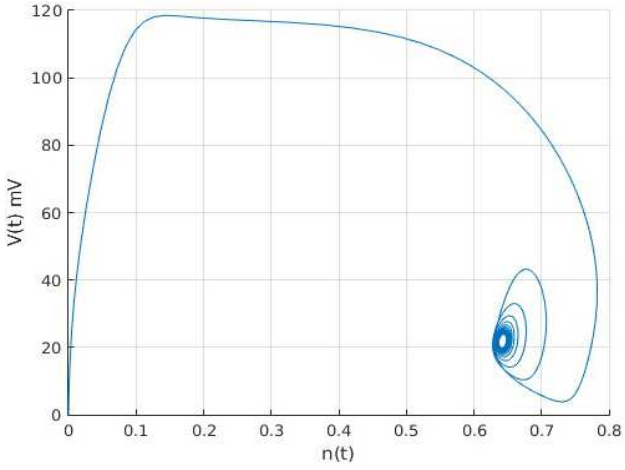

Figure 4b. Case 2: $I_{ext} = 118.351$

Figure 4. Trajectories of the membrane potential $V_m(t)$ and $n(t)$ around the instant of Hopf bifurcations for the cases in Table 1. In (a) a large amplitude Limit Cycle erupts from a subcritical bifurcation of Case 1 as shown. The trajectory has a very small decaying behavior whereas in (b) a smaller amplitude Limit Cycle corresponding to Case 2 is seen. This has a decaying amplitude resulting from a supercritical bifurcation. The steady state value of the limit cycle is almost one tenth of the case in (a).

Control Approaches

As discussed in Section 1, there are numerous approaches in bifurcation control some of which can be classified as washout filters, linear delayed feedbacks, nonlinearity cancellations and intelligent methods such as neural networks. In this research we will discuss the simple linear feedbacks of the form:

$$T(t) = K_o V_m(t) \tag{6}$$

where $T(t)$ is the temperature of the neural environment which serves as an input of the neuron model and K_o is a feedback gain which places the eigenvalues of the Jacobian of the closed loop to a stable location. Here the Jacobian of the closed loop is the Jacobian of (4) combined with (6):

$$\begin{aligned} C_m \frac{dV_m}{dt} &= -\eta(K_o V_m(t))\bar{g}_K n^4 (V_m - V_K) - \eta(K_o V_m(t))\bar{g}_{Na} m^3 h (V_m - V_{Na}) \\ &\quad -\eta(K_o V_m(t))\bar{g}_l (V_m - V_l) + I_{ext} \\ \frac{dn}{dt} &= \phi(K_o V_m(t))\alpha_n(V_m)(1-n) - \phi(K_o V_m(t))\beta_n(V_m) n \\ \frac{dm}{dt} &= \phi(K_o V_m(t))\alpha_m(V_m)(1-m) - \phi(K_o V_m(t))\beta_m(V_m) m \\ \frac{dh}{dt} &= \phi(K_o V_m(t))\alpha_h(V_m)(1-h) - \phi(K_o V_m(t))\beta_h(V_m) h \end{aligned} \tag{7}$$

$$A_c = \begin{bmatrix} \frac{\partial \dot{V}_m}{\partial V_m} & \frac{\partial \dot{V}_m}{\partial n} & \frac{\partial \dot{V}_m}{\partial m} & \frac{\partial \dot{V}_m}{\partial h} \\ \frac{\partial \dot{n}}{\partial V_m} & \frac{\partial \dot{n}}{\partial n} & \frac{\partial \dot{n}}{\partial m} & \frac{\partial \dot{n}}{\partial h} \\ \frac{\partial \dot{m}}{\partial V_m} & \frac{\partial \dot{m}}{\partial n} & \frac{\partial \dot{m}}{\partial m} & \frac{\partial \dot{m}}{\partial h} \\ \frac{\partial \dot{h}}{\partial V_m} & \frac{\partial \dot{h}}{\partial n} & \frac{\partial \dot{h}}{\partial m} & \frac{\partial \dot{h}}{\partial h} \end{bmatrix} \tag{8}$$

The above should be evaluated at the bifurcation equilibrium values presented in **Table 1**. The eigenvalues of A_c will determine the allowable ranges of K_o. There is one additional constraint on the selection of K_o which is the temperature input $T(t)$ to the neuron. This is a major limitation on the control action as high temperature levels (higher than 50) may harm the neuron in actual operation.

Controlling the Bifurcations in HH Model

The purpose of the control here is to implement a feedback so that the bifurcation ceases in the closed loop. In this section we will form the feedback shown in (6) and select values for K_o that will yield eigenvalues of the closed loop formed by (8) and the gain K_o ($\lambda_i(A_c)$) having negative real parts.

Table 2. Equilibria and eigenvalues of A_c in (8) at the gain levels $K_o = \{0.2, 0.4, 0.6, 0.8, 1.0\}$ for Case 1

K_0	0.2	0.4	0.6
Equ.	$V_m = 4.7715$ $n = 0.3926$ $m = 0.0913$ $h = 0.4261$	$V_m = 4.6485$ $n = 0.3907$ $m = 0.0901$ $h = 0.4304$	$V_m = 4.5337$ $n = 0.3888$ $m = 0.0889$ $h = 0.4344$
$\lambda_i(A_c)$	$\lambda_1 = -3.0476 + j0.0000$ $\lambda_2 = -0.0251 + j0.3753$ $\lambda_3 = -0.0251 - j0.3753$ $\lambda_4 = -0.0753 + j0.0000$	$\lambda_1 = -3.2956 + j0.0000$ $\lambda_2 = -0.0515 + j0.4061$ $\lambda_3 = -0.0515 - j0.4061$ $\lambda_4 = -0.0828 + j0.0000$	$\lambda_1 = -3.5519 + j0.0000$ $\lambda_2 = -0.0793 + j0.4363$ $\lambda_3 = -0.0793 - j0.4363$ $\lambda_4 = -0.0906 + j0.0000$
K_0	0.8	1.0	
Equ.	$V_m = 4.4261$ $n = 0.3871$ $m = 0.0879$ $h = 0.4382$	$V_m = 4.3250$ $n = 0.3855$ $m = 0.0869$ $h = 0.4417$	
$\lambda_i(A_c)$	$\lambda_1 = -3.8169 + j0.0000$ $\lambda_2 = -0.1083 + j0.4661$ $\lambda_3 = -0.1083 - j0.4661$ $\lambda_4 = -0.0988 + j0.0000$	$\lambda_1 = -4.0908 + j0.0000$ $\lambda_2 = -0.1385 + j0.4955$ $\lambda_3 = -0.1385 - j0.4955$ $\lambda_4 = -0.1073 + j0.0000$	

Case 1: Hopf ($I_{ext} = 6.686$)

Choosing K_o values as $K_o = \{0.2, 0.4, 06, 0.8, 1.0\}$ yielded the equilibria and eigenvalues (the eigenvalues of A_c in (8)) shown in Table 2.One should note that all represented eigenvalues have negative real parts which means that the chosen gains K_o yielded stable closed loops. However, the range $K_o < 0.2$ did not stop the Hopf bifurcation and the range $K_o > 1.0$ yielded unstable outcome. The membrane potential response and simulated temperature inputs for two limiting cases i.e. $K_o = 0.2$ and $K_o = 1.0$ are presented in Figure 13. Both gain levels are satisfactory to achieve the goals of this research however the required temperature input levels when $K_o = 1$ is extremely high. Better temperature levels are obtained when $K_o \leq 0.6$.

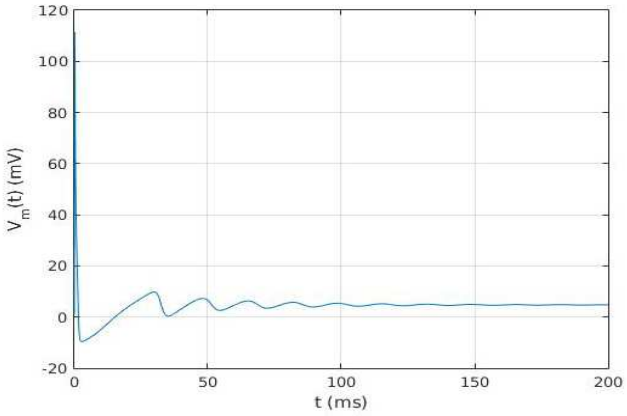

Figure 5a. Case 1: Membrane potential $V_m(t)$ with $K_o = 0.2$

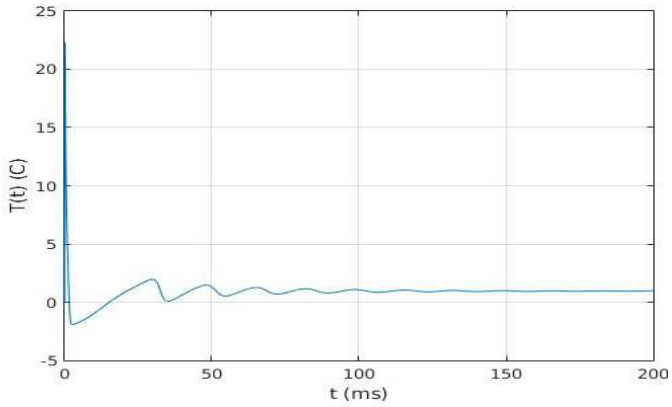

Figure 5b. Case 1: Temperature $T(t)$ with $K_o = 0.2$

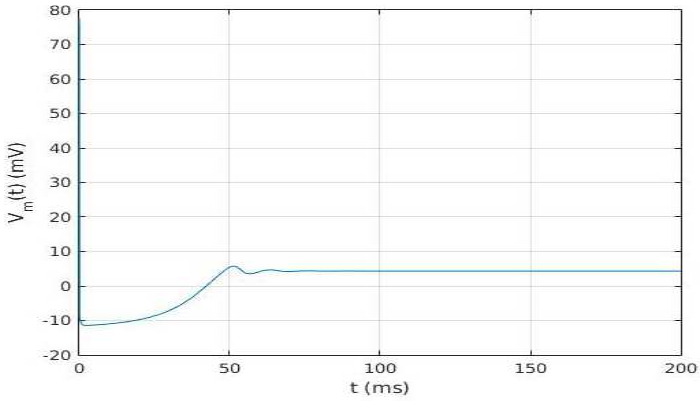

Figure 5c. Case 1: Membrane potential $V_m(t)$ with $K_o = 1.0$

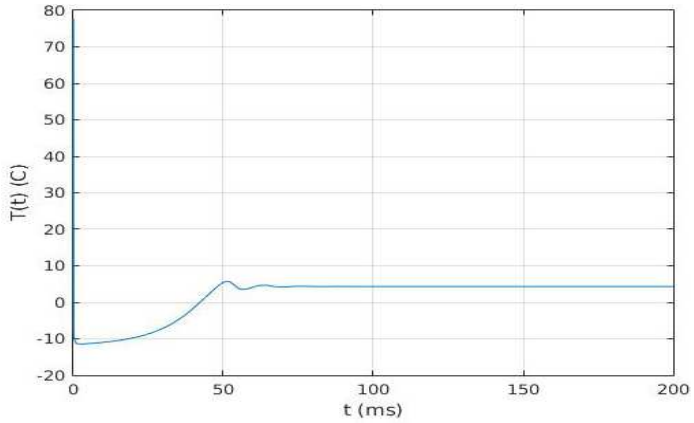

Figure 5d. Case 1: Temperature $T(t)$ with $K_o = 1.0$

Figure 5. Graphical results of bifurcation control of Case 1 $(I_{ext} = 6.686)$ with $K_o = 0.2$ and $K_o = 1.0$. Note the rise in the temperature requirement with the increasing gain K_o.

Results up to this point showed that one is eligible to find a suitable K_o value for implementing a linear control loop to suppress the membrane potential bursts resulting from Hopf phenomena due to changing external current injections.

Here, it will also be interesting to analyze what happens when the external current injection level deviates from its current value. In other words what happens to our closed loop controllers behavior, if the external current injection level changes from $I_{ext} = 6.686\,\mu$ A $/cm^2$ to some other value. One may observe new/additional bifurcation or singularity conditions due to this deviation.

When one has a lower gain like $K_o = 0.2$, the deviation from the original current injection value at $I_{ext} = 6.686\,\mu$ A$/cm^2$ leads to the bifurcation phenomena in Figure 14 and Table 3. It is obvious from the results that, we have 4 critical points (2 Hopf bifurcations one Limit Point and one Neutral Saddle). In addition to the types, one should note that the locations of these 4 critical points span a large range $-12 < I_{ext} < 150$.

Another important result which is directly related to linear stability, is presented in Figure 15. This is the variation of the real part of the maximum eigenvalue of the Jacobian of (7) at a range of I_{ext} values. This is important to see whether the equilibrium point at the analyzed value of I_{ext} is stable or not. What clearly seen from this illustration is that, the eigenvalues associated with the equilibrium points appearing between two Hopf points (this corresponds to the interval $8.426 \le I_{ext} \le 112.323$) are locally unstable as at least one eigenvalue has a positive real part. Here, one will have to change the value of K_o to decrease the range of I_{ext} that leads to instability.

To enlighten this discussion, it would be beneficial to analyze the case where one has a large value of K_o. In the case that $K_o = 1$, the associated bifurcation diagram will be something like Figure 16. The critical points appear here are very close to each other. Thus, one should refer to Table 3 to see the exact locations of the points. From the same table, it should also be noted that there are no Hopf points.

In addition, here it is interesting to note that the real part of the maximum eigenvalue of the Jacobian of (7) stays at the left hand side of the complex plane except at a very small region $-0.843 \le I_{ext} \le -3.259$.

It is pretty normal to face the fact that the real part of the maximum eigenvalue is bi-valuated. We repeat the bifurcation analysis procedure to detect whether there will be any issues when the value of I_{ext} deviate from the design value. Of course there will be instabilities when the same value of K_o is used at different I_{ext} values (other than $I_{ext} = 6.686$). However, when large controller gains are applied the region of instability diminishes. However, for this case gains larger than $K_o = 1.0$ should be avoided as it appeared to be unstable and no further analysis is possible.

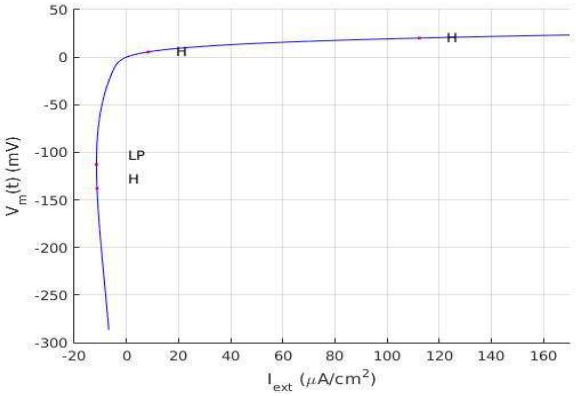

Figure 6a. Case 1: Bifurcation Diagram of (7) for $K_o = 0.2$

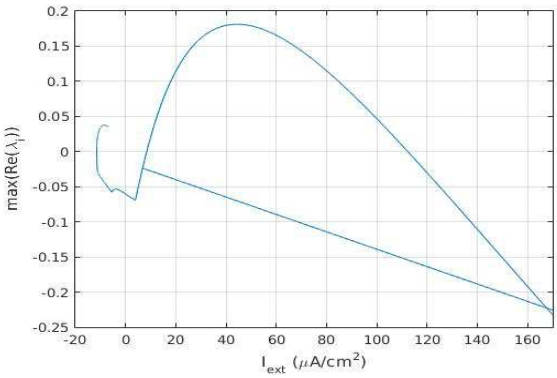

Figure 6b. Case 1: $Re\,(\max\,(\lambda_i(A_c)))$ for $K_o = 0.2$

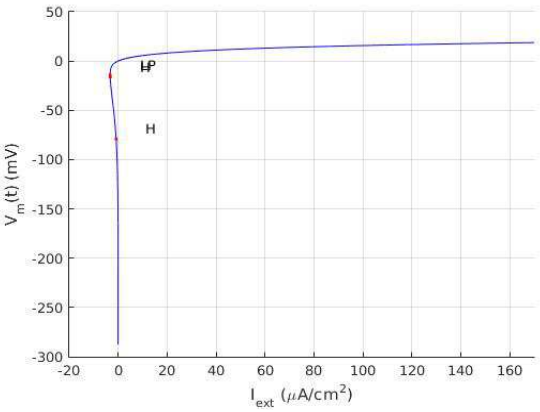

Figure 6c. Case 1: Bifurcation Diagram of (7) for $K_o = 1.0$

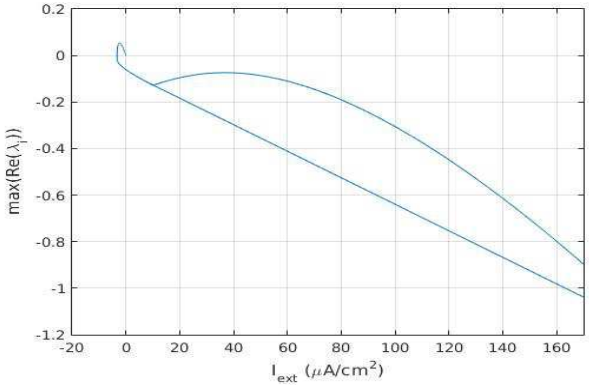

Figure 6d.Case 1: $Re(\max(\lambda_i(A_c)))$ for $K_o = 1.0$

Figure 6. Repeating the bifurcation analysis helps to understand whether the closed loop may initiate new bifurcations at nearby points. Two limiting situations are presented for Case 1 ($I_{ext} = 6.686$) . $K_o = 0.2$ and $K_o = 1.0$.

Table 3. The locations of new bifurcation phenomena due to deviation from the value $I_{ext} = 6.686$ μ A/cm^2 where the control law (temperature law $T(t) = K_o V_m(t)$) is designed and tested. The analysis is made while the control is applied (feedback loop closed). This table is presented to accompany **Figure 14** and **Figure 16**. Labels are: H: Hopf, LP: Limit Point, NS: Neutral Saddle

$K_o = 0.2$			$K_o = 1$		
New Value of I_{ext}	Equilibrium	Type	New Value of I_{ext}	Equilibrium	Type
$I_{ext} = 8.426$	$V_m = 5.574$ $n = 0.405$ $m = 0.0997$ $h = 0.398$	H	$I_{ext} = -3.259$	V_m=–14.05 n=0.138 m=0.0091 h=0.921	P
$I_{ext} = 112.323$	$V_m = 20.088$ $n = 0.620$ $m = 0.371$ $h = 0.0865$	H	$I_{ext} = -3.239$	V_m=–16.57 n=0.115 m=0.0065 h=0.944	S
$I_{ext} = -11.489$	$V_m = -112.702$ $n = 0.0$ $m = 0.0$ $h = 1.0$	LP	$I_{ext} = -0.843$	$V_m = -79.136$ $n = 0.00035$ $m = 0.0$ $h = 0.9999$	S
$I_{ext} = -11.28$	$V_m = -137.74$ $n = 0.0$ $m = 0.0$ $h = 1.0$	NS			

Table 4. Equilibria and eigenvalues of A_c in (8) at the gain levels $K_o = \{0.05, 0.1, 0.3, 0.5, 0.8, 1.0, 1.2\}$ for Case 2.

K_0	0.05	0.1	0.3	0.5
Equ.	$V_m = 21.4830$ $n = 0.6377$ $m = 0.4076$ $h = 0.0740$	$V_m = 21.1354$ $n = 0.6334$ $m = 0.3985$ $h = 0.0770$	$V_m = 19.8765$ $n = 0.6175$ $m = 0.3661$ $h = 0.0886$	$V_m = 18.7923$ $n = 0.6033$ $m = 0.3388$ $h = 0.1001$
Eig.	$\lambda_1 = -7.6605 + j0.0000$ $\lambda_2 = -0.0043 + j0.6149$ $\lambda_3 = -0.0043 - j0.6149$ $\lambda_4 = -0.1712 + j0.0000$	$\lambda_1 = -8.1745 + j0.0000$ $\lambda_2 = -0.0096 + j0.6736$ $\lambda_3 = -0.0096 - j0.6736$ $\lambda_4 = -0.1887 + j0.0000$	$\lambda_1 = -10.3312 + j0.0000$ $\lambda_2 = -0.0431 + j0.9470$ $\lambda_3 = -0.0431 - j0.9470$ $\lambda_4 = -0.2707 + j0.0000$	$\lambda_1 = -12.6808 + j0.0000$ $\lambda_2 = -0.1037 + j1.2856$ $\lambda_3 = -0.1037 - j1.2856$ $\lambda_4 = -0.3739 + j0.0000$
K_0	0.8	1.0	1.2	
Equ.	$V_m = 17.4126$ $n = 0.5848$ $m = 0.3053$ $h = 0.1170$	$V_m = 16.6207$ $n = 0.5738$ $m = 0.2868$ $h = 0.1279$	$V_m = 15.9106$ $n = 0.5638$ $m = 0.2707$ $h = 0.1386$	
Eig.	$\lambda_1 = -16.6621 + j0.0000$ $\lambda_2 = -0.2663 + j1.9212$ $\lambda_3 = -0.2663 - j1.9212$ $\lambda_4 = -0.5738 + j0.0000$	$\lambda_1 = -19.6889 + j0.0000$ $\lambda_2 = -0.4355 + j2.4306$ $\lambda_3 = -0.4355 - j2.4306$ $\lambda_4 = -0.7406 + j0.0000$	$\lambda_1 = -23.0732 + j0.0000$ $\lambda_2 = -0.6620 + j3.0062$ $\lambda_3 = -0.6620 - j3.0062$ $\lambda_4 = -0.9369 + j0.0000$	

The results in Figure 18 and Table 3 showed that larger gains (like $K_o = 1.0$) lead to a safer closed loop. When the gain is lower such as $K_o = 0.2$, the deviations of I_{ext} from the design value 6.686 led to 4 bifurcation phenomena at various locations as shown in the first column of Table 3. In addition Figure 15 showed that, at least one of the eigenvalues stay at the left hand side of the complex plane which is a sign of loss of local stability of the equilibrium point. On the other hand, when one has a comparably larger gain like $K_o = 1.0$ the critical points or bifurcations appear in a very narrow band of $-3.529 \leq I_{ext} \leq -0.843$. Also from Figure 17, it

should be noted that the real part of the maximum eigenvalue stays negative for a very large region of I_{ext}. So one can say that, increasing the control gain K_o helps improving the robustness of the bifurcation controller.

Case 2: Hopf ($I_{ext} = 118.351$)

In this section we will repeat the analysis and simulation steps of Section 3.3.1. The control gain K_o is chosen from the set $K_o = \{0.05, 0.1, 03, 0.5, 0.8, 1.0, 1.2\}$. The equilibria and eigenvalue results are shown in Table 4. All of these gains yield stable closed loops. However, when $K_o < 0.05$ the controller is unsuccessful in prevention of the bifurcation for Case 2 and when the gain is larger than $K_o = 1.2$ the neuron becomes unstable. The goals are obtained by using a small gain like $K_o = 0.05$. This is an expected situation as Case 2 is an example of a supercritical bifurcation. The response of the closed loop for the two limiting values of the gains $K_o = 0.05$ and $K_o = 1.2$ are shown in Figure 23.

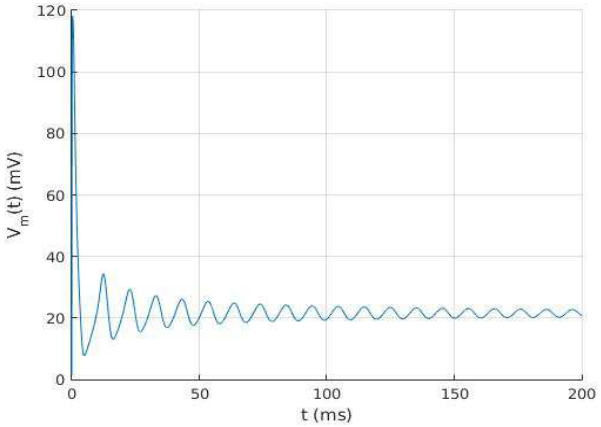

Figure 7a. Case 2: Membrane potential $V_m(t)$ with $K_o = 0.05$

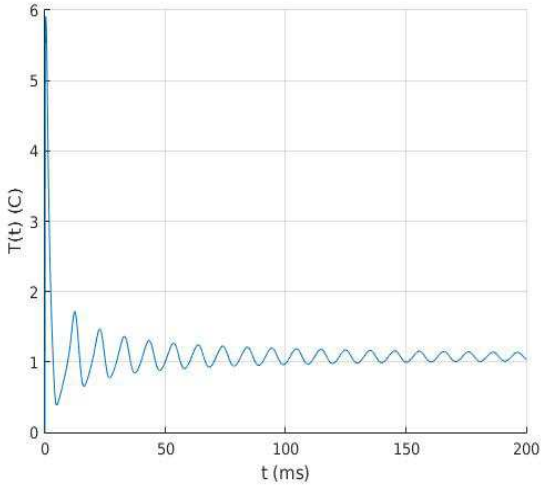

Figure 7b. Case 2: Temperature $T(t)$ with $K_o = 0.05$

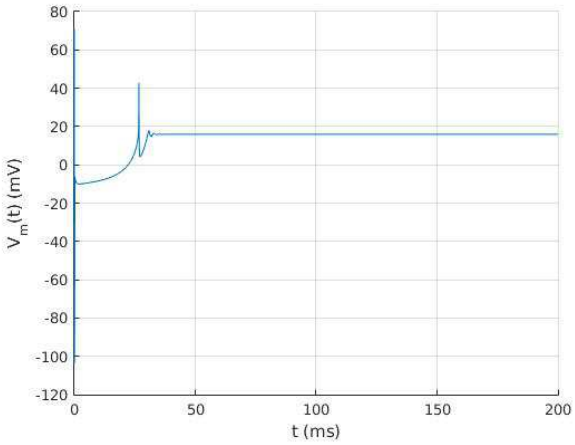

Figure 7c. Case 2: Membrane potential $V_m(t)$ with $K_o = 1.2$

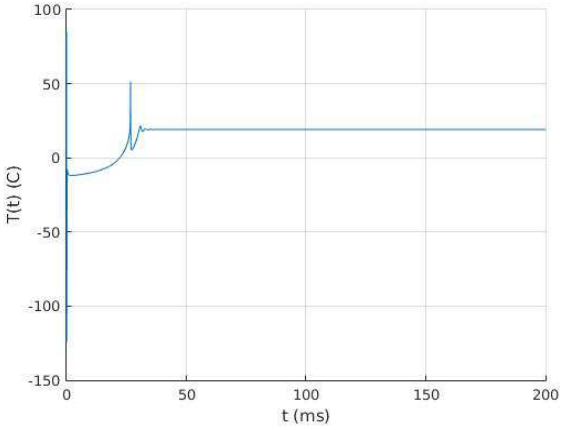

Figure 7d. Case 2: Temperature $T(t)$ with $K_o = 1.2$

Figure 7. Graphical results of bifurcation control of Case 2 $(I_{ext} = 118.351)$ with $K_o = 0.2$ and $K_o = 1.0$. Note the rise in the temperature requirement with the increasing gain K_o

It is understood from Figure 23 that, the temperature input requirement stays at or below 50. Like that of Case 1, it will also be beneficial to repeat the bifurcation analysis for the closed loop against I_{ext} values deviated from the design value $I_{ext} = 118.351$.

When the control gain is smaller such as $K_o = 0.05$. The deviation of I_{ext} from the value 118.351 leads to the bifurcation conditions in the diagram of Figure 24 which shows that there are two Hopf cases. The exact locations and types of points can be clearly seen in Table 5. Similar to that of Case 1, there is a fairly large range of instability which is in $7.058 \le I_{ext} \le 117.099$ (See Figure 25). Similar to that of Case 2, the bifurcations will appear in a very small interval $-2.934 \le I_{ext} \le -1.228$ when the control gain is increased to $K_o = 1.2$ (Figure 26). Associated with this result, the region of instability is also diminished as revealed from Figure 27. In short, we can say that the results associated with the closed loop bifurcation analysis of Case 1 and Case 2 of Table 1 are compatible. This is an expected result. When the gains are increased the instability region against varying values of I_{ext} contracts.

Gains larger than $K_o = 1.2$ should be avoided in stabilization of the Hopf bifurcation when $I_{ext} = 118.351$. Larger values leads to instabilities.

One can see the associated results for the situation of $K_o = 0.05$ and $K_o = 1.2$ in Figure 28. Similar to that of Case 1, possible bifurcation conditions due to varying I_{ext} shifts to farther locations (moved to left on the graph). In addition, the larger the gain K_o larger the region that

closed loop eigenvalues stay in the negative left half plane.

Table 5. The locations of new bifurcation phenomena due to deviation from the value $I_{ext} = 118.351$ μ A/cm^2 of Case 2, where the control law (temperature law $T(t) = K_o V_m(t)$) is designed and tested. The analysis is made while the control is applied (feedback loop closed). This table is presented to accompany Figure 24 and Figure 26. Labels are: H: Hopf, LP: Limit Point, NS: Neutral Saddle

$K_o = 0.05$			$K_o = 1.2$		
New Value of I_{ext}	Equilibrium	Type	New Value of I_{ext}	Equilibrium	Type
$I_{ext} = 7.058$	$V_m = 5.056$ $n = 0.397$ $m = 0.094$ $h = 0.416$	H	$I_{ext} = -2.9430$	$V_m = -11.356$ $n = 0.165$ $m = 0.012$ $h = 0.886$	LP
$I_{ext} = 117.099$	$V_m = 21.396$ $n = 0.636$ $m = 0.405$ $h = 0.074$	H	$I_{ext} = -2.9342$	$V_m = -12.624$ $n = 0.152$ $m = 0.011$ $h = 0.905$	NS
			$I_{ext} = -1.228$	$V_m = -50.206$ $n = 0.006$ $m = 0.00006$ $h = 0.999$	NS

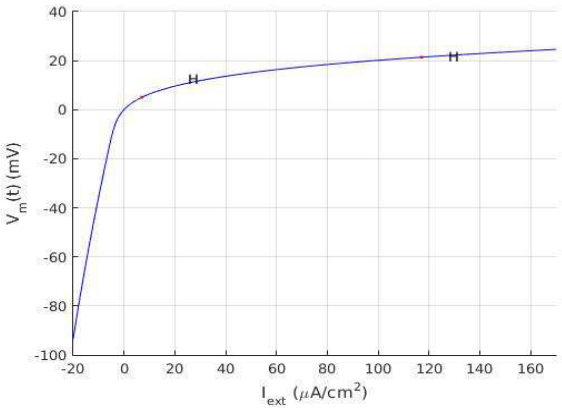

Figure 8a. Case 2: Bifurcation Diagram of (7) for $K_o = 0.05$

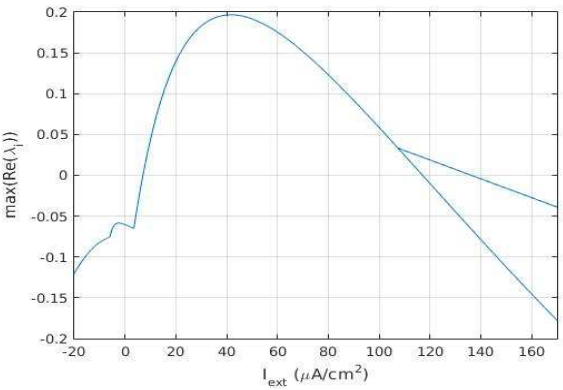

Figure 8b. Case 2: $Re(\max(\lambda_i(A_c)))$ for $K_o = 0.05$

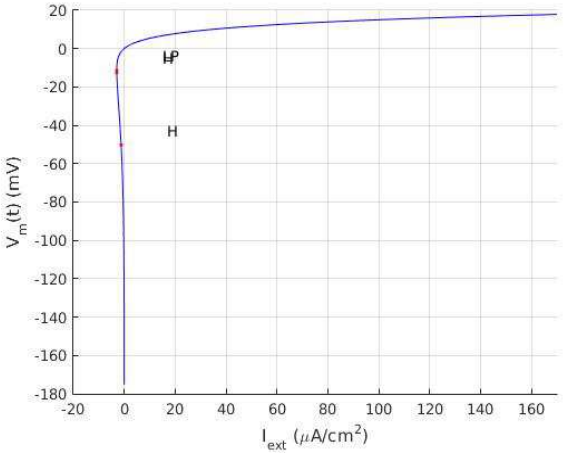

Figure 8c. Case 2: Bifurcation Diagram of (7) for $K_o = 1.2$

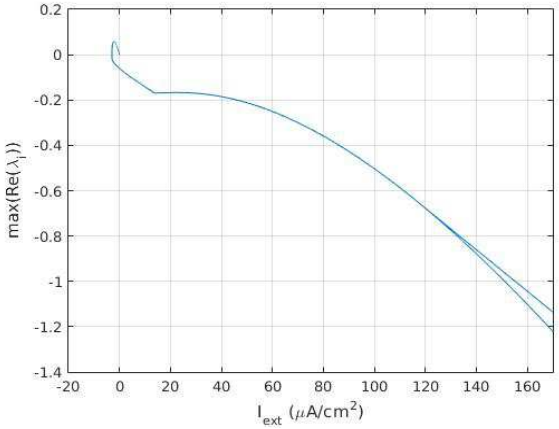

Figure 8d. Case 2: $Re(\max(\lambda_i(A_c)))$ for $K_o = 1.2$

Figure 8. The bifurcation analysis of the closed loop for Case 2 $(I_{ext} = 118.351)$ with the feedback gains $K_o = 0.05$ and $K_o = 1.2$.

Conclusion

We have presented a theoretical application of bifurcation control by linear feedback to the stabilization of oscillations in the Hodgkin-Huxley neurons due to Hopf bifurcations. The source of bifurcations (bifurcating parameter) in our model is the external current injections (I_{ext}) which is also the case in various sources found in literature. However, in this work we obtain the control action by manipulating the temperature of the environment where the neuron is functioning. The study is divided into three main parts. In the first part, we analyzed the bifurcations by a software package called as MATCONT which is an open source third party MATLAB toolbox. It is understood that, when external current injection I_{ext} is varied two Hopf bifurcations are detected (see Table 1). There are one subcritical and one supercritical bifurcation cases (Figure 6 and Figure 7 respectively). In the second part of this reserach, we have developed a linear control law that only feeds information from membrane potential through a gain. For each case in Table 1, a set of feedback gains K_o ranging from $K_o = 0.05$ to $K_o = 1.2$ are examined both by eigenvalue checking and simulation. In the case of subcritical Hopf bifurcation $(I_e xt = 6.686)$, the suitable control gain appeared to be in the range of $0.2 \le K_o \le 1.0$. The simulations performed with a larger gain $(K_o > 1.0)$ lead to an instability. For the supercritical Hopf case, successful ranges of K_o appear to be in range $0.05 \le K_o \le 1.2$. Similar to the subcritical case,

simulations performed with an out-of-range gain ($K_o > 1.2$) results in an unstable closed loop. In the given ranges all simulations yielded stable outcomes as shown in Figures 13, 23. In the simulations, there were a momentary temperature rise over 100 but the duration is so small that is not considered an issue (even in a biological application).

As a companion to the study of the controllers for each case of bifurcation in Table 1 we repeat the analysis when the loop is closed. In Table 2 and Figure 4, the control gains are tested at the two bifurcation conditions presented in Table 1. However, there may be the cases where the external current injection level I_{ext} deviates from the values listed in the table. The software MATCONT is invoked again while the loop is closed. When one has a low control gain ($K_o = 0.2$ for Case 1 and $K_o = 0.05$ for Case 2 from Table 1), the variation of I_{ext} led to additional critical points presented in Figure 14and Figure 24. The results showed that, critical points may appear in a large range of I_{ext} when one has a lower gain. When one has a large gain ($K_o = 1.0$ for Case 1 and $K_o = 1.2$ for Case 2 from Table 1), the associated results will be as in Figure 16 and Figure 26. Those reveal that, large gains lead to critical situations in a very narrow range of I_{ext}. The significance of this analysis becomes apparent when one observes the variation of the sign of the real part of the maximum eigenvalue of the closed loop formed by Jacobian of (7) and the temperature control law in (6) against varying I_{ext}. This information is available in Figure 15 and Figure 25 for lower control gains and in Figure 17 and Figure 27 for large gains. It is obvious from those presentations is that, lower gains lead to a large region of instability whereas when larger gains applied this region appeared to be very narrow.

References

Abbott LF. Theoretical neuroscience rising. Neuron 2008;60(3):489-95.

Abed EH, Wang HO, Chen RC. Stabilization of period doubling bifurcations and implications for control of chaos. Physica D: Nonlinear Phenomena. 1994;70(1-2):154-64.

Abrams R. Electroconvulsive therapy. Oxford University Press, 2002.

Andronov AA, Leontovich EA, Gordon II, Maier AG. Qualitative theory of second-order dynamic systems. 1973.

Ayala GF, Dichter M, Gumnit RJ, Matsumoto H, Spencer WA. Genesis of epileptic interictal spikes. New knowledge of cortical feedback systems suggests a neurophysiological explanation of brief paroxysms. Brain Research 1973;52:1-7.

Berns DW, Moiola JL, Chen G. Feedback control of limit cycle amplitudes from a frequency domain approach. Automatica 1998;34(12):1567-73.

Brandt ME, Chen G. Bifurcation control of two nonlinear models of cardiac activity. IEEE Transactions on Circuits and Systems I: Fundamental Theory and Applications 1997;44(10):1031-34.

Cheng Z. Anti-control of Hopf bifurcation for Chen's system through washout filters. Neurocomputing 2010;73(16):3139-46.

Crawford JD. Introduction to bifurcation theory. Reviews of Modern Physics 1991;63(4):991.

Dhooge A, Govaerts W, Kuznetsov YA. MATCONT: a MATLAB package for numerical bifurcation analysis of ODEs. ACM Transactions on Mathematical Software (TOMS) 2003;29(2):141-64.

Dimitrijevic MR, Sherwood AM, Nathan PW. Clonus: peripheral and central mechanisms. Progress in Clinical Neurophysiology Prog Clin Neurophysiol 1978;5:173-82.

Ding L, Hou C. Stabilizing control of Hopf bifurcation in the Hodgkin–Huxley model via washout filter with linear control term. Nonlinear Dynamics 2010;60(1-2):131-39.

Doruk RO. Control of repetitive firing in Hodgkin–Huxley nerve fibers using electric fields. Chaos, Solitons & Fractals 2013;52:66-72.

Doruk RÖ. Washout filter based control for the Hodgkin-Huxley nerve cell dynamics. Turkısh Journal of Electrıcal Engıneerıng & Computer Scıences 2010;18(4):553-70.

Feudel U, Neiman A, Pei X, Wojtenek W, Braun H, Huber M, Moss F. Homoclinic bifurcation in a Hodgkin–Huxley model of thermally sensitive neurons. Chaos: An Interdisciplinary Journal of Nonlinear Science 2000;10(1):231-39.

Fitzhugh R. Theoretical effect of temperature on threshold in the Hodgkin-Huxley nerve model. The Journal of General Physiology 1966;49(5):989-1005.

Forster FM. Reflex epilepsy, behavioral therapy, and conditional reflexes. Charles C Thomas Pub Limited, 1977.

Glaser GH, Penry JK, Woodbury DM, editors. Antiepileptic drugs: Mechanisms of action. Epilepsy Society, 1980.

Harb AM, Harb BA. Chaos control of third-order phase-locked loops using backstepping nonlinear controller. Chaos, Solitons & Fractals 2004;20(4):719-23.

Hassouneh MA, Lee HC, Abed EH. Washout filters in feedback control: Benefits, limitations and extensions. InAmerican Control Conference, 2004. Proceedings of the 2004;5:3950. IEEE.

Hodgkin AL, Huxley AF. A quantitative description of membrane current and its application to conduction and excitation in nerve. The Journal of Physiology 1952;117(4):500-44.

Hong KS. Hopf bifurcation control via a dynamic state-feedback control. Physics Letters A 2012;376(4):442-46.

Kang W. Bifurcation and normal form of nonlinear control systems, Part I. SIAM Journal on Control and Optimization 1998;36(1):193–212.

Kuznetsov YA. Elements of applied bifurcation theory, volume 112. Springer Science & Business Media, 2013.

Lee HC, Abed EH. Washout filters in the bifurcation control of high alpha flight dynamics. In American Control Conference, 1991:206-211. IEEE.

Liao X, Wong KW, Leung CS, Wu Z. Hopf bifurcation and chaos in a single delayed neuron equation with non-monotonic activation function. Chaos, Solitons & Fractals 2001;12(8):1535-47.

Luo XS, Chen G, Wang BH, Fang JQ. Hybrid control of period-doubling bifurcation and chaos in discrete nonlinear dynamical systems. Chaos, Solitons & Fractals 2003;18(4):775-83.

Marsden C. Origins of normal and pathological tremor. In Movement disorders: tremor. Springer, 1984: 37–84.

Marsden CD. The pathophysiology of movement disorders. Neurologic clinics Clinics 1984;2:435-59.

Milton JG, Gotman J, Remillard GM, Andermann F. Timing of seizure recurrence in adult epileptic patients: a statistical analysis. Epilepsia 1987;28(5):471-78.

Milton JG, Longtin A, Beuter A, Mackey MC, Glass L. Complex dynamics and bifurcations in neurology. Journal of Theoretical Biology 1989;138(2):129-47.

Peng M. Multiple bifurcations and periodic "bubbling" in a delay population model. Chaos, Solitons & Fractals 2005;25(5):1123-30.

Rinberg A, Taylor AL, Marder E. The effects of temperature on the stability of a neuronal oscillator. PLoS Computational Biology 2013;9(1):e1002857.

Sterman MB, Friar L. Suppression of seizures in an epileptic following sensorimotor EEG feedback training. Electroencephalography and Clinical Neurophysiology 1972;33(1):89-95.

Vidyasagar M. Nonlinear systems analysis. Prentice Hall, 1978.

Wang J, Chen L, Fei X. Analysis and control of the bifurcation of Hodgkin–Huxley model. Chaos, Solitons & Fractals 2007;31(1):247–256.

Wang J, Chen L, Fei X. Bifurcation control of the Hodgkin–Huxley equations. Chaos, Solitons & Fractals 2007;33(1):217-24.

Wehr TA, Goodwin FK. Circadian rhythms in psychiatry, volume 2. Boxwood Press, 1983.

Xie Y, Chen L, Kang YM, Aihara K. Controlling the onset of Hopf bifurcation in the Hodgkin-Huxley model. Physical Review E 2008;77(6):061921.

Zhou L, Tang Y, Hussein S. Stability and Hopf bifurcation for a delay competition diffusion system. Chaos, Solitons & Fractals 2002;14(8):1201-25.